

The Veinot group developed a convenient and versatile method for synthesizing Si-NCs that involves thermal treatment of an electronics grade, sol-gel derived silicon rich oxide resin that only contains Si, O, and H.⁷ This high purity precursor minimizes the possibility of impurities while still allowing for the incorporation of dopants.⁴¹ The Si-NC size is conveniently tuned by defining the maximum processing temperature and/or time.⁴² Furthermore, this method is readily transferrable to other laboratories. With a modest infrastructure investment in a high temperature tube furnace, high purity Si-NCs can be prepared using equipment and techniques common to most synthetic chemistry laboratories.

The general procedure affords freestanding particles with dimensions ranging from a few to hundreds of nanometers; however, most studies focus on Si-NCs 15 nm in diameter or less.^{7,42} In addition, a variant of this method, which is beyond the scope of this contribution, provides highly luminescent Si-NC/SiO₂ thin films that are readily patterned or incorporated into optical structures.⁴³

The preparation of Si-NCs using silicon rich oxide precursors was first introduced by Liu et al. whereby silicon suboxide powders (SiO_x, $x = 0.4-1.8$) were thermally annealed in inert atmosphere at 900 °C.⁴⁴ After HF etching, freestanding hydride terminated Si-NCs were obtained with a mean diameter of 4.2 nm. This provided a platform for the development of the method described in this paper: the thermal processing of commercially available hydrogen silsesquioxane (HSQ, HSiO_{1.5}) under a slightly reducing atmosphere to obtain Si-NCs in bulk quantities.⁷ This method, and variants thereof, has been embraced by numerous researchers^{32,45-49} to reproducibly generate high quality Si-NCs of varying sizes.

A significant challenge associated with elemental Si-NCs is the propensity to oxidize in the presence of air and water.⁵⁰ Oxidation diminishes the reactive hydride surface, destroys the crystallinity and can influence photoluminescence intensity. However, oxidation can be minimized by covalent functionalization of ligands to the surface.^{39,51} The covalent linkage is robust and enhances the stability of the particles toward oxidation. In addition, there is a wide array of functional groups that can be used for surface functionalization. This allows both the physical (e.g., solution processability) and optical properties to be tuned.⁵² For example, orange-emitting 3 nm Si-NCs can be made to luminesce blue when functionalized by an amine^{53,54} or red when an alkyl group is attached to the surface.^{9,54}

Covalent surface functionalization requires the creation of a reactive particle surface. Building on the pioneering work of Chidsey,⁵⁵ Buriak,^{56,57} and others^{26,58-60} involving bulk and porous silicon, hydride (or hydrogen) termination is the most common starting point,^{35,52,61-63} although chloride^{28,29,31} and hydroxyl terminations⁶⁴ have also been reported. Surface modifications of Si-NCs that employ hydride-based starting materials typically involve reactions with terminal alkenes or alkynes and are initiated by heat,⁶⁵ UV irradiation,⁶⁶ a Lewis acid,⁶⁷ or a radical source.^{68,69} However, interactions of the particle surface with amines,⁵³ alcohols⁷⁰ and carboxylic acids⁵¹ have also been reported. The functionalization of hydride-terminated Si-NCs is an excellent starting point as well as an area of expertise within our group and will be discussed herein.

The effectiveness of the high temperature processing of HSQ to form high purity Si-NCs is highlighted by its use in various groups and the developments that have been made as a result (e.g., light-emitting diodes, Si-NC superlattices, sensors, and responsive materials).^{16,71-74}

Using a silicon-rich oxide as a starting point this article details the steps needed to ultimately obtain functionalized Si-NCs. To begin, we highlight the procedure for synthesizing pure, near monodisperse Si-NCs of well-defined size and their liberation using HF etching. Subsequently the discussion will shift to various methods used to functionalize Si-NCs. For illustrative purposes, dodecene is used as a representative example for the passivation (functionalization) of the Si-NC surface. Finally, the most common characterization methods will be discussed and representative data from each will be presented.

■ PARTICLE SYNTHESIS

The Veinot group method for synthesizing Si-NCs is based on high temperature processing of hydrogen silsesquioxane (HSQ). HSQ is a commercially available silicon rich oxide (HSiO_{1.5}) that is commonly used as an electron-beam resist and spin-on dielectric. It disproportionates when heated in a slightly reducing atmosphere to form SiO₂ and Si. Thermal processing begins by loading a reaction vessel containing HSQ into a high temperature tube furnace. A reducing atmosphere is created by flowing a gas consisting of 5% H₂/95% Ar through the tube. The temperature is then ramped to the target end point and held for a designated dwell time and finally cooled to room temperature. Note that the ramp rate is set based upon the manufacturer specifications and is dependent on the composition and diameter of the work tube. The elemental Si subsequently clusters to form nanocrystals encapsulated in a SiO₂ matrix (Scheme 1, HSQ-composite). The size of the oxide embedded particles is dependent on both the temperature and dwell time (see Table 1).

Scheme 1. High Temperature Processing of HSQ To Form a Composite Consisting of Si-NCs Embedded in a SiO₂ Matrix

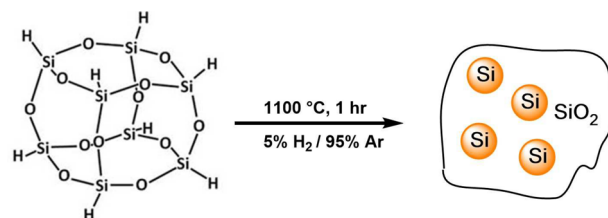


Table 1. Nominal Annealing Temperatures and Dwell Times for the Synthesis of Si-NCs of Various Diameters

Si-NC diameter (nm)	temperature (°C)	dwell time (hours)
3	1100	1
6	1200	1
9	1300	1

Before starting the procedure to make Si-NCs, be sure to consider the compatibility of your furnace work tube with the conditions given in Table 1. For example, a quartz tube is suitable for heating to 1100 °C but softens above this temperature; temperatures at or above 1200 °C require alumina or zirconia tubes. One must also determine if the tube is compatible with the reducing atmosphere as the tube itself may become reduced. A quartz tube is inert to the reducing atmosphere but a nonpassivated alumina tube may lead to unintended metallic aluminum impurities. If the furnace tube specifications are appropriate for reaching high temperatures (up to 1500 °C) and it is inert toward the 5% H₂/95% Ar atmosphere, particles described herein can be prepared directly in a single furnace tube. Otherwise, the preparation of particles of greater than 3 nm

requires two steps. First, 3 nm particles are produced via heating to 1100 °C under reducing conditions. The resulting composite is then transferred to a more thermally resistant tube and heated in Ar at the desired temperature to increase the particle size. (Note: Samples are placed in reaction boats within the tube, the boat composition is typically the same as the furnace work tube.)

Once furnace logistics are resolved, the synthesis can be performed. The HSQ should be a moderately fine and consistent powder; grind if necessary. HSQ is added to reaction boats and should be distributed uniformly throughout (Supporting Information S1.a). For best results, the boat should not be filled to more than half of its depth. The size of the boat will be limited by the diameter of the tube in the furnace. More than one boat may be filled and loaded into the furnace tube simultaneously depending on the size and heat profile of the furnace being used. To ensure best that the HSQ is exposed to a stable temperature, care should be taken to ensure the boats are within the maximum heating zone (Supporting Information S1.b); some furnaces contain plugs to help stabilize the internal temperature. Finally, in the event that multiple boats are loaded, ensure that the boats are not in contact with each other to allow for temperature and gas flow stability.

Gas flow is monitored using a bubbler connected downstream of the furnace work tube. A bubble rate of ca. 1 mL/s has proven most effective and it is imperative that the gas remains flowing throughout the processing procedure. The bubble rate may increase at maximum temperature as gaseous silanes are formed. These silanes are reactive and flammable and therefore the bubbler must be vented in a fume hood. In our experience combustion of silanes is rarely observed.

After holding at the desired temperature for the appropriate time, the sample is cooled under gas flow. *Do not take steps to cool the furnace rapidly!* Rapid cooling may damage the working tube and will affect the quality of the composite. Once the temperature drops below 50 °C, the composite can be safely removed from the furnace work tube. If effective thermal processing has occurred, the composite should have a shiny black appearance and may have fused into larger chunks. The resulting product (i.e., composite) consists of Si-NCs embedded within a protective silica matrix and may be safely handled in air. However, both personal protective equipment and a well-ventilated fume hood are recommended as airborne particulates may be present. To liberate the Si-NCs the silica must be removed via HF etching. However, the as prepared composite is not suitable for effective HF etching. The surface area must be increased and the grains must be of a reasonably uniform size.

■ GRINDING

The composite is ground manually using an agate mortar and pestle. The composite is covered with ethanol during the grinding process (Supporting Information S1.c and video). The ethanol prevents dust formation and as the grain size is decreased the composite suspends in ethanol and allows for straightforward removal from larger grains. It is strongly advised that a dust mask and fume hood be utilized while grinding. The light brown suspension that forms can be removed using a Pasteur pipet and transferred to a thick walled, pear shaped 500 mL glass flask containing 5 mm diameter glass beads. Larger particles that settle from the ethanol slurry require further manual grinding prior to subsequent suspension and transferring to the flask. Additional ethanol may be added to the slurry as needed. In general, 5 g of composite requires approximately 100 mL of ethanol. The flask is capped and shaken using a standard wrist action shaker for a

minimum of 6 h. The resulting pretreated composite is readily collected using a Buchner apparatus. Sonication with ethanol can be employed to remove composite adhering to the flask wall. Allow the composite to fully dry before storage. Special storage requirements are not required; samples of composite can be safely kept in a standard screw-top vial until needed in the etching step (Supporting Information S1.d).

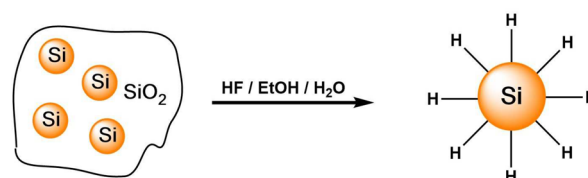
■ ETCHING

Etching is performed with a commercial aqueous 49% HF solution. *Caution: Solutions of HF are extremely hazardous!* In our research group, a designated laboratory and fume hood is used and all personnel undergo extensive training. In addition, calcium gluconate gel and benzalkonium chloride are readily available at all times. Rigorous safety precautions and personal protective equipment protocols are strictly followed.⁷⁵ Local regulations must be consulted prior to using HF. Teflon lab equipment is used for all HF manipulations and cleanup of all HF containing solutions is performed using concentrated solutions of CaCl₂.

Other etching procedures have been reported in the literature. Most significant among them is the use of HCl/HF,⁷⁶ which provides faster etching. However, there is the possibility of chloride contamination that can adversely affect optical response and subsequent reactivity of the Si-NCs.⁸ For the purposes of this paper, a standard HF etching procedure will be described. In a typical experiment, 0.5 g of shaker-ground composite is weighed into a 50 mL Teflon beaker equipped with a Teflon coated stir bar. Five ml of ethanol is added to the composite with sonication to ensure a uniform suspension is achieved (Supporting Information S2.a); this typically takes about 1 min. 5 mL of water is then added and further sonication (about 30 s) is performed (if composite quantity is varied, use ~1 mL of each solvent per ~0.1 g of composite).

The addition of 5 mL of 49% HF solution (the volume of HF will be equivalent to the amount of water) and commencement of stirring initiates the etching process (Scheme 2, NP composite

Scheme 2. Production of Hydride Terminated Si-NCs by HF Etching of the Si-NC Composite



to free-standing particles). The initial brown suspension will change in color and appear light yellow-orange over time; this is a qualitative indication of complete etching (Supporting Information S2.b). Etching times vary between 0.5 and 1 h depending on effectiveness of grinding. The completion of etching should be judged based on visual evidence as opposed to solely on time.

The etching is quenched by adding approximately 20 mL of toluene and stirring to suspend the hydrophobic hydride terminated particles in the toluene layer (Supporting Information S2.c). If the etch was efficient, there should be negligible evidence of solids in the aqueous HF layer. The toluene layer appears as a suspension of orange particles and the aqueous layer should be clear/colorless. The top toluene layer, containing hydride terminated Si-NCs, is then carefully removed using a plastic pipet and transferred to glass test tubes. The extraction procedure is repeated until the upper layer is clear, signifying

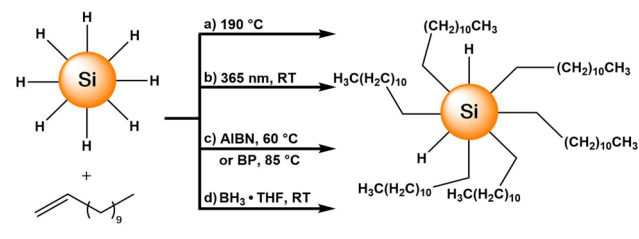
complete extraction of the Si-NCs. At this point, the Si-NCs are freestanding and will exhibit characteristic luminescence under exposure to UV light. The test tubes containing the Si-NC in toluene suspension are then centrifuged at 3000 rpm for 10 min. This yields a clear solution with the particles forming a tight pellet at the bottom of each tube (Supporting Information S2.d). The extracted toluene will contain traces of water that will lead to particle oxidation. Therefore, the supernatant toluene is removed using a Pasteur pipet. The resulting hydride-terminated particles can then be redispersed in the dry organic solvent of choice, although alcohols are a notable exception and should be avoided. The particles are then transferred to a clean, dry Schlenk flask prefilled with argon.

A freeze-drying technique is employed if dry particles in powder form are required. In this case, the particles should be dispersed in dry benzene and transferred to a clean, dry Schlenk flask that has been charged with argon. The suspension is frozen using liquid nitrogen and a vacuum is applied to the flask (Supporting Information S2.e). The liquid nitrogen Dewar is removed and the benzene is sublimed *in vacuo* to yield an orange powder (Supporting Information S2.f). The freeze-drying procedure is typically used when subsequent reactions require the use of a glovebox or the functionalization reaction involves a water, or air, sensitive ligand.

■ PARTICLE FUNCTIONALIZATION

There are numerous methods outlined throughout the literature for functionalizing Si-NCs.^{8,9,52,62,67,77–80} Typically, these involve activating surface Si–H bonds to create a reactive silicon surface in the presence of a ligand of choice, resulting in the formation of a robust Si–C covalent bond between the ligand and the surface. The most commonly used ligands possess a terminal olefin and the functionalization proceeds via addition of the Si–H bond across the C=C bond. The ligand can be changed to not only change the pendant functional group but also to define the surface linkage.^{9,52,80–84} For the purposes of this paper, four common functionalization methods will be highlighted using 1-dodecene as the prototypical ligand (Scheme 3, functionalization routes). As hydride-terminated Si-NCs are

Scheme 3. Formation of Dodecene Functionalized Si-NCs by (a) Thermal, (b) Photo, (c) Radical Initiated, and (d) Lewis Acid Initiated Reactions



sensitive to oxidation by air and, especially, water, great care is taken to ensure exposure is minimized during the functionalization process. This is crucial, as oxidation will be most prevalent when the hydride terminated Si-NCs are activated during the functionalization process. As such, standard Schlenk protocols are used (Supporting Information S3.a) with glassware oven-dried at 125 °C and all solvents used in the reactions are dried and purified using a solvent purification system. Three freeze/pump/thaw cycles are also performed prior to performing the reaction in order to remove trace oxygen (Supporting

Information S3.b). If the reagent to be used for functionalization is not stored under inert conditions, it should be added before performing the freeze/pump/thaw cycles.

Freshly etched hydride-terminated particles are dispersible in organic solvents such as toluene and THF. These particle dispersions exhibit a cloudy yellow appearance and will settle over time. Functionalization of Si-NCs creates an outer protective shell, leading to sterically stabilized colloids and compatibility with common solvents. For example, when 1-dodecene is used as the ligand the pendant end is an alkane making the particle nonpolar in much the same way as an alkane. As a result, in toluene the hydride-terminated particles are transformed from a cloudy yellow dispersion to a transparent orange-yellow solution of dodecene functionalized particles. This qualitative observation is the first indication that a successful functionalization has occurred. As a general rule, smaller particles are more easily dispersed in solvents than their larger counterparts. For example, 3 nm particles form transparent solutions in toluene whereas larger (i.e., 6 nm or greater) particles result in cloudy systems. If a polar ligand such as pentenoic acid is used, the pendant end is a carboxylic acid. In toluene, evidence of a successful functionalization is the observation of a clear, colorless solution with Si-NC precipitate either adhering to the walls of the flask and/or rapidly settling to the bottom of the reaction vessel.

■ THERMALLY INDUCED HYDROSILYLATION

Thermally induced hydrosilylation occurs between the Si–H surface and a terminal alkene and is initiated by heating the reaction mixture to ca. 190 °C. Because of the high temperature requirement, attention must be paid to the choice of solvents and ligands used. The boiling point (bp) of 1-dodecene is 213.8 °C and it is a liquid at room temperature. Thus, it is ideal for the thermal reaction as it can serve both as ligand and solvent. Alternatively, solvents such as *p*-dichlorobenzene (bp = 173 °C) have been used with other high boiling ligands such as 9-decen-1-ol (bp = 234–238 °C). For our representative ligand, freeze-dried or centrifuged Si-NCs are dispersed into ca. 20 mL of neat 1-dodecene in a dry Schlenk flask backfilled with argon and equipped with a Teflon coated magnetic stir bar. This results in a cloudy yellow suspension. Three cycles of evacuation and backfilling with argon are performed. The reaction mixture is then heated to 190 °C and stirred overnight under argon. A transparent orange-yellow solution is typically observed.

Microwave reactors may also be used to carry out thermal reactions. The reaction vial is sealed and pressures of up to 10 bar can be accommodated. Thus, temperatures well above boiling may be used. This allows the use of lower boiling ligands and solvents such as toluene or THF. Consult the user manual for the maximum solvent temperatures and pressures applicable to each microwave reactor.

■ RADICAL AND LEWIS ACID-INITIATED HYDROSILYLATION

Radical initiated hydrosilylation is advantageous as it requires relatively mild conditions. Two primary radical initiators have been used for hydrosilylation. Azobis(isobutyronitrile) (AIBN) and benzoyl peroxide are used in catalytic amounts (~5% by weight based on mass of composite used) and require gentle heating (60 °C for AIBN and 85 °C for benzoyl peroxide). Borane (1.0 M in THF) is a Lewis acid initiator and requires equimolar amounts with respect to the ligand but the reaction

can be carried out at room temperature. For these reactions, Si-NCs are dispersed in the dry solvent of choice (typically toluene) and transferred to a dry, argon filled Schlenk flask equipped with a Teflon coated magnetic stir bar. An excess of previously dried 1-dodecene is then added to the cloudy yellow suspension. For example, 3 mL of dodecene is suitable for a reaction starting with 0.25 g of Si-NC composite. Three freeze–pump–thaw cycles are then performed. Finally, the radical or Lewis acid initiator of choice is added to the reaction mixture. As these are either dry solids or solutions stored under dry, inert conditions, no further drying or purification is necessary. With stirring, the reaction mixture is heated as defined by the initiator used. As with the thermal method, after time the reaction mixture becomes a transparent orange-yellow solution. Typical reaction times are at least 6 h as the radical initiators, especially AIBN, require an activation period.

■ PHOTOCHEMICAL HYDROSILYLATION

Si-NCs have a Bohr exciton radius of 5 nm. Below this threshold, quantum size effects occur. These effects give rise to unique characteristics such as visible photoluminescence. However, quantum confinement also impacts photochemical reactions in that exciton mediated reactions such as photochemical hydrosilylation are restricted for particles greater than 5 nm in diameter.¹¹

Photochemical hydrosilylation reactions are carried out in Schlenk flasks equipped with quartz inserts that can hold house-made 365 nm, 450 mW UV LED probes (2 LEDs per probe, purchased from Nichia Corporation, Tokyo, Japan) (Supporting Information S3.c). These reactant mixtures are prepared in the same way as those used in radical or Lewis acid initiated reactions; however, no initiator is added. Once the freeze–pump–thaw cycles are complete the UV LEDs are inserted and turned on to initiate the reaction (Supporting Information S3.d). The reaction vessel is wrapped in aluminum foil or another UV resistant protective barrier to prevent exposure to stray UV light. Reaction time is typically a minimum of 6 h although this time may be shortened if a more intense UV source is used.

■ PURIFICATION

Functionalized Si-NC purification is performed using a solvent/antisolvent washing method. The goal is to have a solvent combination in which the excess ligand is soluble but the particles are not readily dispersible. The functionalized Si-NCs are successively washed and centrifuged in order to remove excess starting material and other impurities. The dodecane functionalized Si-NCs are dispersible in toluene and, if the reaction was performed in neat dodecane, the particles will be highly dispersible. Purification for dodecane functionalized Si-NCs requires the addition of a polar antisolvent, typically ethanol or methanol. A 1:1 mixture of ethanol and methanol may also be used. A minimum of 50% antisolvent is required, however, depending on how stable the particles are in solution, a higher proportion of antisolvent may be required. Upon addition of antisolvent, the sample typically becomes less transparent as the particles destabilize in solution. The sample is then centrifuged at 12000 rpm for 20–30 min to form a solid pellet at the bottom of the centrifuge tube. These parameters can be adjusted based on the capabilities of the centrifuge and the properties of the sample and solution system. The supernatant is removed and the particles are dispersed in a small amount of solvent. Antisolvent is added followed by mixing and centrifuging again. The particles

must be redispersed in the fresh solvent before centrifuging for effective washing. This washing sequence is typically performed a total of three times. Finally, the functionalized Si-NCs can be dispersed in the solvent of choice for storage, usually toluene for nonpolar functionalities. As the Si-NCs are now passivated special storage precautions are typically not required and simple storage in a vial is sufficient (Supporting Information S3.e). The final sample may also be filtered through a 0.45 μm PTFE syringe filter to remove large aggregates. This general procedure is applicable to all particle functionalities but the choices of solvents and antisolvent will vary based on the type of ligand as this changes the polarity of the functionalized particles.

Each of the functionalization methods described here have been shown to be effective (Table 2). However, care must be

Table 2. Summary of the Advantages and Disadvantages of the Various Functionalization Methods

func. method	advantages	disadvantages
thermal	1. most complete surface coverage	1. oligomerization 2. solvent/reagent compatibility 3. high boiling solvents required
radical	1. wide array of ligands 2. different si linkages	1. nonspecific functionalization 2. potential impurity from catalyst
Lewis acid	1. wide array of ligands 2. room temperature	1. incompatible with alcohols 2. large amount required
photochemical	1. only ligand and Si-NCs present	1. limited suitable reagents 2. restricted to 5 nm or less Si-NCs
microwave	1. withstand high pressure 2. low boiling solvents can be used	1. specialized instrumentation 2. precipitation may cause vial breakage

taken to choose the appropriate method according to the type of functionalization required. The thermal method tends to give the most complete surface coverage but oligomerization has been observed with long chain alkenes. Also, the thermal method is not readily compatible with low boiling or thermally unstable solvents or ligands. The microwave method is a closed system that can tolerate moderately high pressures allowing the use of lower boiling components. Aside from the requirement for specialized instrumentation best results are obtained for samples that form well dispersed systems as excessive precipitation may cause localized heating and lead to vial breakage. Radical initiators are effective for use with a wide array of ligands and can create different linkages to the surface such as Si–N and Si–O bonds. However, if the ligand of choice has two reactive ends (e.g., 9-decen-1-ol), both may react with the particle causing a mixed functionalization. Lewis acid mediated reactions are not catalytic and a relatively large amount of borane is required. Normally, this is not a deterrent; but if an alcohol is present, a large excess of borane is needed to overcome the preferential interaction with the alcohol before the functionalization can occur. Photochemical hydrosilylation does not introduce impurities in the form of additional reagents but it is not compatible for all ligands. Ligands that photodegrade or polymerize are not effective with this method. Also, photochemical reactions are only effective in reacting alkenes with the silicon surface for nanocrystals less than 5 nm in diameter.

Photochemical activation is advantageous if one must prevent pendant groups such as alcohols or carboxylic acids from attaching to the surface.

CHARACTERIZATION

Characterization of Si-NCs can be challenging. A recent commentary outlined the essential information needed for a full and complete characterization of inorganic nanomaterials.⁸⁵ To characterize suitably a functionalized nanocrystal, one must gain information regarding particle composition, size and shape, extent and orientation of surface functionality, and the physical or optical properties. It is fair to consider characterization of nanocrystals as a puzzle. No one single technique provides an unambiguous confirmation of the structure; multiple complementary techniques must be used together to provide as clear a picture as possible. Full particle analysis is time-consuming and expensive. Fortunately, it may not be necessary to apply every characterization technique to every sample, especially if a series of similarly functionalized particles are to be synthesized. The following section does not go into detail about each technique. Rather, it is intended to help the researcher to minimize extraneous characterization and understand the requirements for full characterization (Table 3).

Table 3. Summary of the Information Obtained from the Primary Si-NC Characterization Techniques

characterization technique	information obtained
XRD	establish crystallinity, estimate particle diameter from composite
photoluminescence	evaluate quality of etched particles
IR	evaluate extent of functionalization
XPS	measure particle oxidation and presence of heteroatoms
TEM	establish particle diameter and size distribution
SAXS	particle diameter and size distribution of suspensions
DLS	hydrodynamic radius of particles in suspension

A key component to nanocrystal synthesis is size. For the purposes of this paper, size is synonymous with diameter as all of the particles described here are pseudospherical. X-ray diffraction (XRD) is a relatively straightforward and rapid way to effectively determine the quality of a Si-NC/SiO₂ composite prepared using the presented procedure and can be used to establish the consistency of a new particle synthesis method. The first indication of Si-NC size is obtained from the ground composite via XRD. The XRD peaks, which are representative of the lattice planes of the crystalline Si-NC, broaden as the particle diameter decreases (Figure 1) and the Scherrer equation can then be applied to determine the diameter.⁸⁶ If the XRD shows only amorphous character (i.e., no reflections indicating the Si lattice planes are present), this is an indication that Si-NCs did not form.

Photoluminescence (PL) spectroscopy, due to its straightforward and nondestructive nature, is invaluable in monitoring and evaluating Si-NCs of less than 5 nm. Particles of larger diameters can be seen by PL spectroscopy if near IR detection is available (Figure 2). PL spectroscopy cannot be used as a standalone technique but it does provide useful information during the course of an experiment. Using a UV light deck or portable UV penlight, a quick check of PL of a suspension of freshly etched 3 nm hydride terminated Si-NCs in toluene shows emission in the orange-red region of the visible spectrum. The observation of PL indicates that the Si-NCs are not fully oxidized or dissolved away.

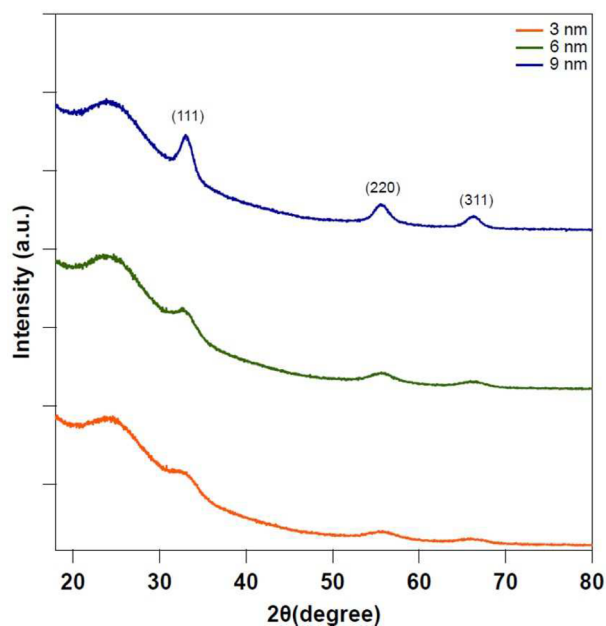


Figure 1. X-ray diffraction curves for composites of 3, 6, and 9 Si-NCs within SiO₂ matrices. Characteristic (111), (220), and (311) reflections of the Si diamond lattice are identified. The broad peak at 20° is due to amorphous SiO₂.

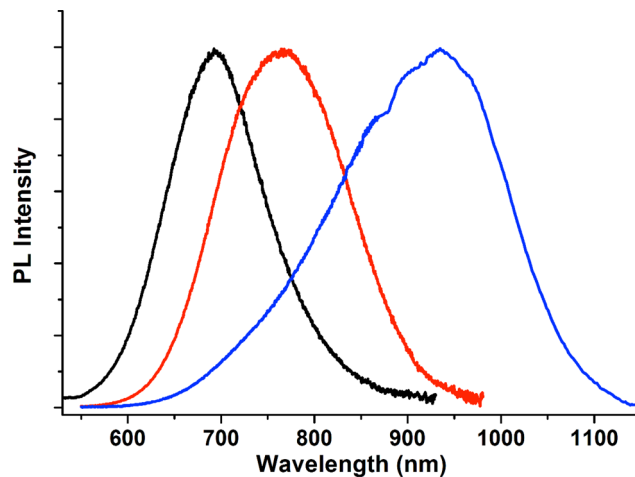


Figure 2. Photoluminescence spectroscopy spectra of 3 nm (black), 6 nm (red), and 9 nm (blue) dodecane functionalized Si-NC.

In some cases, PL can give a crude indication of particle size in that smaller particles emit at shorter wavelengths but researchers should be cautioned that other factors, such as surface groups, contribute to the wavelength of emission. In our laboratory, PL is used routinely to follow the course of a functionalization reaction as functionalized particles often show emission at a different wavelength than hydride-terminated particles. (This quick visual check is not applicable to particles 5 nm or greater in diameter.) Note that some ligands cause quenching of the PL, which can also be used as evidence of a reaction. As always, one must be aware that luminescence may not always be due to the presence of Si-NCs as many molecular species also emit under UV light; observation of PL alone should not be considered as definitive proof of a reaction.

A great deal of useful information about nanocrystals can be gained by qualitative observations. When performing a large number of related reactions, these observations can help to

reduce the time spent on characterization. For example, freshly etched hydride terminated Si-NCs in toluene are a cloudy yellow suspension but form a transparent yellow solution after functionalization with dodecane. Conversely, after functionalization with a polar end group such as $-\text{COOH}$, the particles are completely insoluble in toluene but readily disperse in ethanol. One can often surmise if the reaction appears successful allowing for the decision to proceed with further characterization.

After functionalization, infrared spectroscopy (IR) serves as the front-line technique and is performed on virtually every sample. Although IR is suited for molecular species, it can be useful in evaluating the particle surface and, hence, the functionalization. It is imperative that before an IR spectrum is obtained, that the Si-NCs are purified to remove excess ligand from the sample. It is crucial to know if the ligand peaks in the IR are from the free ligand or from those attached to the particle surface. If the particles are washed effectively, the likely answer becomes that they are attached. The main signals for the hydride terminated Si-NCs are attributed to $\text{Si}-\text{H}_x$ ($x = 1, 2, 3$; ca. 2100 cm^{-1}) and $\text{Si}-\text{O}$ (ca. 1065 cm^{-1}) bands. After functionalization, there is a distinct reduction in the relative intensity of the $\text{Si}-\text{H}$ band and the appearance of bands characteristic to the ligand. The intensity of the $\text{Si}-\text{O}$ band can be used as an approximate guide to the level of surface oxidation that occurs during functionalization and workup. The IR spectra for the hydride terminated Si-NCs and dodecane functionalized particles are shown in Figure 3 and illustrate these expected changes.

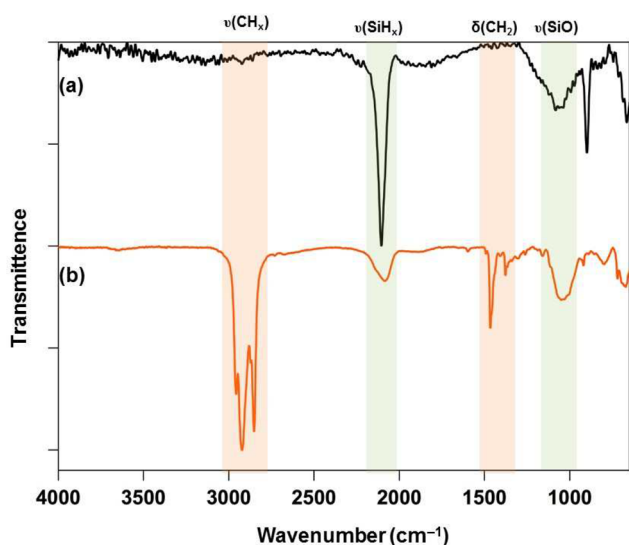


Figure 3. IR spectroscopy spectra for (a) freshly etched hydride terminated Si-NCs and (b) dodecane functionalized Si-NCs.

Spectrum A shows the presence of oxide upon etching, but it should be noted that near oxide-free Si-NCs can be obtained if appropriate care is taken. Limited information is available from IR spectra thus agreement between the qualitative observations (e.g., solubility) and the IR data is typically required before proceeding with other more involved techniques.

X-ray photoelectron spectroscopy (XPS) is performed periodically on samples that show promise based on the previously described characterizations. In our laboratory, XPS is not used as a survey technique. Rather, it is typically used periodically to establish and verify the progress of research and is predominantly used once experimental procedures are properly established and the work is nearing publication. XPS allows for

the elemental composition of the nanocrystals, including the surface ligands, to be identified. Therefore, if there is a unique element such as N or F in the ligand, the presence of this element in the XP spectrum typically indicates that functionalization has occurred. XPS also gives an indication of the extent of oxidation but it is less sensitive than FT-IR for this purpose. Fitting of high resolution XPS data provides further information regarding oxidation states, which can in turn indicate connectivity. Information regarding the level of oxidation of Si can also be cross-referenced by inspecting the intensity of the $\text{Si}-\text{O}-\text{Si}$ band in the IR spectrum. The XP spectrum and subsequent fitting using Casa software⁸⁷ for 3 nm Si-NCs functionalized with dodecane is shown in Figure 4.

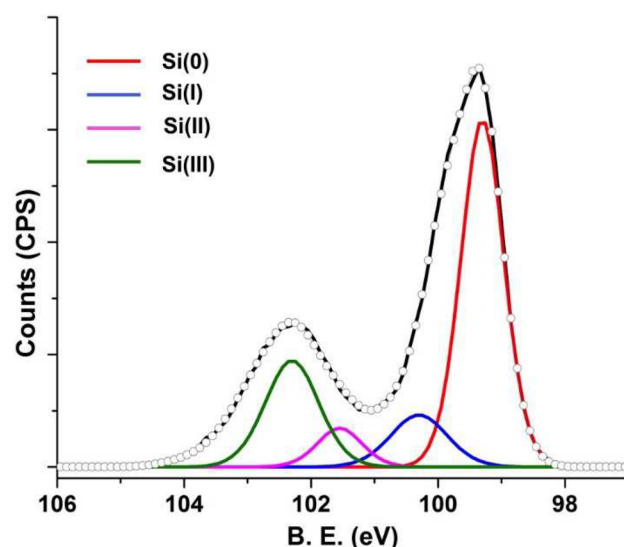


Figure 4. X-ray photoelectron plot of dodecane functionalized Si-NCs (black line). The various oxidation states of silicon that are present (colored lines) are determined by fitting.

Depending on the nature of the research, the final characterization method is transmission electron microscopy (TEM). Representative TEM images along with particle size distributions determined using ImageJ software⁸⁸ are shown in Figure 5. TEM

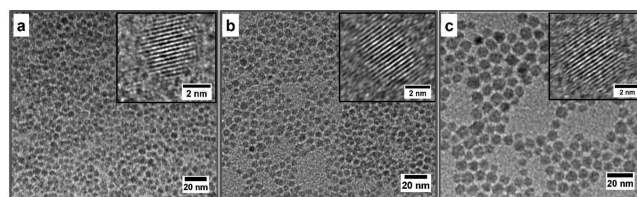


Figure 5. Bright field transmission electron microscopy images with accompanying high resolution TEM and size distribution graphs for (a) 3 nm, (b) 6 nm, and (c) 9 nm and dodecane functionalized Si-NCs.

is exceedingly valuable as it not only confirms the core size and shape but allows for the determination of size distribution. TEM is both costly and labor/time intensive to run and inexperienced users may be prone to overinterpreting the data. For example, aggregation can be caused during sample preparation and/or crystallization can occur in the electron beam. As a result the images may not be representative of the original sample. Furthermore, Si-NCs can be difficult to distinguish from the background due to their small size and relatively low contrast. The value of a TEM image increases greatly when combined with

energy dispersive X-ray (EDX), which provides elemental analysis of the particle core and functional groups. Lattice spacing can also be determined which further confirms the identity of the particle core.

Alternatively, particle sizing can be performed using small-angle X-ray scattering (SAXS).¹¹ SAXS measurements are made using dilute suspensions of nanomaterials and provides quantitative particle diameter and distribution data. SAXS measurements are rapid and require minimal sample preparation. However, careful mathematical fitting of the data is required for analysis. In some cases, particle sizing in solution (hydrodynamic diameter) is more important than the core size. This is often the case for biological or environmental research. In these cases, dynamic light scattering (DLS) is a valuable tool. DLS is far more straightforward and much more inexpensive to perform compared to TEM. There is no aggregation due to sample drying; however, DLS requires the particles to undergo Brownian motion, which can be difficult to achieve with samples that disperse poorly.

CONCLUSIONS

Si-NCs produced using high temperature processing of HSQ are of high purity with a tunable and narrow size distribution. As these particles provide a blank canvas, the effects of impurities, surface groups, particle size, or the origin of luminescence can be studied. These particles can then be functionalized using a number of different methods; the method chosen based on the numerous potential ligands and surface functionalities. Reliable characterization of functionalized Si-NCs is both crucial and challenging. A sensible and practical approach to characterization enhances the efficiency of our research without compromising on quality. Carefully established experimental and characterization procedures such as those described in this paper provide a basis for successful synthesis of functionalized Si-NCs. These procedures can be adapted in a cost efficient way to be utilized in most inorganic synthetic laboratories. Si-NCs continue to show promise in commercial applications and we consider the contributions of our lab as one of many in advancing fundamental Si-NC research.

ASSOCIATED CONTENT

Supporting Information

The Supporting Information is available free of charge on the ACS Publications website at DOI: [10.1021/acs.chemmater.6b02667](https://doi.org/10.1021/acs.chemmater.6b02667).

Photos including HSQ in quartz boat, thermally processed Si-NCs, SiNCs after grinding, Si-NCs in water/ethanol solution, etched Si-NCs prior extraction and partitioned into toluene, 3 nm Si-NCs under ambient and UV light, freeze-drying apparatus, hydride terminated Si-NCs under ambient and UV light, functionalization setup, frozen Si-NCs, photochemical apparatus, SiNCs after functionalization and after washing under UV light and size-distribution histograms of Si-NC from TEM imaging (PDF)
Video demonstrating Si-NC composite grinding procedure (MPG)

AUTHOR INFORMATION

Corresponding Author

*J. G. C. Veinot. Phone: +1-780-492-7206. Fax: +1-780-492-8231. E-mail: jveinot@ualberta.ca.

Notes

The authors declare no competing financial interest.

ACKNOWLEDGMENTS

The authors thank all former members of the Veinot group for their roles in the development of these methods. We thank the Natural Sciences and Engineering Research Council of Canada (NSERC) Discovery Grant Program and the NSERC CREATE supported Alberta/Technical University of Munich International Graduate School for Hybrid Functional Materials (ATUMS) for continued generous financial support. We also thank the Analytical Services and ACSES staff at the University of Alberta for their help with characterization. J. Washington thanks Concordia University of Edmonton for financial support.

ABBREVIATIONS

Si-NCs, silicon nanocrystals; XRD, X-ray diffraction; PL, photoluminescence; IR, infrared; XPS, X-ray photoelectron spectroscopy; TEM, transmission electron microscopy

REFERENCES

- (1) Bhattacharjee, S.; Rietjens, I. M.; Singh, M. P.; Atkins, T. M.; Purkait, T. K.; Xu, Z.; Regli, S.; Shukaliak, A.; Clark, R. J.; Mitchell, B. S.; et al. Cytotoxicity of Surface-Functionalized Silicon and Germanium Nanoparticles: The Dominant Role of Surface Charges. *Nanoscale* **2013**, *5*, 4870–4883.
- (2) Erogbogbo, F.; Yong, K.; Roy, I.; Xu, G.; Prasad, P. N.; Swihart, M. T. Biocompatible Luminescent Silicon Quantum Dots for Imaging of Cancer Cells. *ACS Nano* **2008**, *2*, 873–878.
- (3) Brus, L. Luminescence of Silicon Materials: Chains, Sheets, Nanocrystals, Nanowires, Microcrystals, and Porous Silicon. *J. Phys. Chem.* **1994**, *98*, 3575–3581.
- (4) Pi, X.; Liptak, R.; Nowak, J. D.; Wells, N.; Carter, C.; Campbell, S.; Kortshagen, U. Air-Stable Full-Visible-Spectrum Emission from Silicon Nanocrystals Synthesized by an All-Gas-Phase Plasma Approach. *Nanotechnology* **2008**, *19*, 245603–245607.
- (5) Hessel, C. M.; Reid, D.; Panthani, M. G.; Rasch, M. R.; Goodfellow, B. W.; Wei, J.; Fujii, H.; Akhavan, V.; Korgel, B. A. Synthesis of Ligand-Stabilized Silicon Nanocrystals with Size-Dependent Photoluminescence Spanning Visible to Near-Infrared Wavelengths. *Chem. Mater.* **2012**, *24*, 393–401.
- (6) Ledoux, G.; Gong, J.; Huisken, F.; Guillois, O.; Reynaud, C. Photoluminescence of Size-Separated Silicon Nanocrystals: Confirmation of Quantum Confinement. *Appl. Phys. Lett.* **2002**, *80*, 4834–4836.
- (7) Hessel, C. M.; Henderson, E. J.; Veinot, J. G. Hydrogen Silsesquioxane: A Molecular Precursor for Nanocrystalline Si-SiO₂ Composites and Freestanding Hydride-Surface-Terminated Silicon Nanoparticles. *Chem. Mater.* **2006**, *18*, 6139–6146.
- (8) Dasog, M.; Bader, K.; Veinot, J. G. Influence of Halides on the Optical Properties of Silicon Quantum Dots. *Chem. Mater.* **2015**, *27*, 1153–1156.
- (9) Dasog, M.; Veinot, J. G. Tuning Silicon Quantum Dot Luminescence via Surface Groups. *Phys. Status Solidi B* **2014**, *251*, 2216–2220.
- (10) Kang, Z.; Liu, Y.; Tsang, C. H. A.; Ma, D. D. D.; Fan, X.; Wong, N.; Lee, S. Water-Soluble Silicon Quantum Dots with Wavelength-Tunable Photoluminescence. *Adv. Mater.* **2009**, *21*, 661–664.
- (11) Kelly, J. A.; Shukaliak, A. M.; Fleischauser, M. D.; Veinot, J. G. Size-Dependent Reactivity in Hydrosilylation of Silicon Nanocrystals. *J. Am. Chem. Soc.* **2011**, *133*, 9564–9571.
- (12) Iqbal, M.; Purkait, T. K.; Goss, G. G.; Bolton, J. R.; Gamal El-Din, M.; Veinot, J. G. Application of Engineered Si Nanoparticles in Light-Induced Advanced Oxidation Remediation of a Water-Borne Model Contaminant. *ACS Nano* **2016**, *10*, 5405–5412.
- (13) Kovalev, D.; Fujii, M. Silicon Nanocrystals: Photosensitizers for Oxygen Molecules. *Adv. Mater.* **2005**, *17*, 2531–2544.

- (14) Van Buuren, T.; Dinh, L.; Chase, L.; Siekhaus, W.; Terminello, L. J. Changes in the Electronic Properties of Si Nanocrystals as a Function of Particle Size. *Phys. Rev. Lett.* **1998**, *80*, 3803–3806.
- (15) Yong, K.; Law, W.; Hu, R.; Ye, L.; Liu, L.; Swihart, M. T.; Prasad, P. N. Nanotoxicity Assessment of Quantum Dots: From Cellular to Primate Studies. *Chem. Soc. Rev.* **2013**, *42*, 1236–1250.
- (16) Gonzalez, C. M.; Iqbal, M.; Dasog, M.; Piercey, D. G.; Lockwood, R.; Klapötke, T. M.; Veinot, J. G. Detection of High-Energy Compounds Using Photoluminescent Silicon Nanocrystal Paper Based Sensors. *Nanoscale* **2014**, *6*, 2608–2612.
- (17) Liu, C.; Holman, Z. C.; Kortshagen, U. R. Hybrid Solar Cells from P3HT and Silicon Nanocrystals. *Nano Lett.* **2009**, *9*, 449–452.
- (18) Lalic, N.; Linnros, J. Light Emitting Diode Structure Based on Si Nanocrystals Formed by Implantation into Thermal Oxide. *J. Lumin.* **1998**, *80*, 263–267.
- (19) Puzzo, D. P.; Henderson, E. J.; Helander, M. G.; Wang, Z.; Ozin, G. A.; Lu, Z. Visible Colloidal Nanocrystal Silicon Light-Emitting Diode. *Nano Lett.* **2011**, *11*, 1585–1590.
- (20) Mastronardi, M. L.; Henderson, E. J.; Puzzo, D. P.; Chang, Y.; Wang, Z. B.; Helander, M. G.; Jeong, J.; Kherani, N. P.; Lu, Z.; Ozin, G. A. Silicon Nanocrystal OLEDs: Effect of Organic Capping Group on Performance. *Small* **2012**, *8*, 3647–3654.
- (21) Li, Z.; Ruckenstein, E. Water-Soluble Poly (acrylic acid) Grafted Luminescent Silicon Nanoparticles and their Use as Fluorescent Biological Staining Labels. *Nano Lett.* **2004**, *4*, 1463–1467.
- (22) Ji, X.; Peng, F.; Zhong, Y.; Su, Y.; Jiang, X.; Song, C.; Yang, L.; Chu, B.; Lee, S.; He, Y. Highly Fluorescent, Photostable, and Ultrasmall Silicon Drug Nanocarriers for Long-Term Tumor Cell Tracking and In-Vivo Cancer Therapy. *Adv. Mater.* **2015**, *27*, 1029–1034.
- (23) McVey, B. F.; Tilley, R. D. Solution Synthesis, Optical Properties, and Bioimaging Applications of Silicon Nanocrystals. *Acc. Chem. Res.* **2014**, *47*, 3045–3051.
- (24) Cheng, X.; Lowe, S. B.; Reece, P. J.; Gooding, J. J. Colloidal Silicon Quantum Dots: From Preparation to the Modification of Self-Assembled Monolayers (SAMs) for Bio-Applications. *Chem. Soc. Rev.* **2014**, *43*, 2680–2700.
- (25) Heath, J. R. A Liquid-Solution-Phase Synthesis of Crystalline Silicon. *Science* **1992**, *258*, 1131–1133.
- (26) Wilcoxon, J.; Samara, G. Tailorable, Visible Light Emission from Silicon Nanocrystals. *Appl. Phys. Lett.* **1999**, *74*, 3164–3166.
- (27) Teh, G. B.; Nagalingam, S.; Tilley, R. D.; Ramesh, S.; Lim, Y. S. Colloidal Synthesis of Silicon Nanocrystals via Inverse Micelles Microemulsion. *Z. Phys. Chem.* **2009**, *223*, 1417–1426.
- (28) Bley, R. A.; Kauzlarich, S. M. A Low-Temperature Solution Phase Route for the Synthesis of Silicon Nanoclusters. *J. Am. Chem. Soc.* **1996**, *118*, 12461–12462.
- (29) Mayeri, D.; Phillips, B. L.; Augustine, M. P.; Kauzlarich, S. M. NMR study of the Synthesis of Alkyl-Terminated Silicon Nanoparticles from the Reaction of SiCl₄ with the Zintl Salt, NaSi. *Chem. Mater.* **2001**, *13*, 765–770.
- (30) Liu, Q.; Kauzlarich, S. M. A New Synthetic Route for the Synthesis of Hydrogen Terminated Silicon Nanoparticles. *Mater. Sci. Eng., B* **2002**, *96*, 72–75.
- (31) Pettigrew, K. A.; Liu, Q.; Power, P. P.; Kauzlarich, S. M. Solution Synthesis of Alkyl- and Alkyl/Alkoxy-Capped Silicon Nanoparticles via Oxidation of Mg₂Si. *Chem. Mater.* **2003**, *15*, 4005–4011.
- (32) Holmes, J. D.; Ziegler, K. J.; Doty, R. C.; Pell, L. E.; Johnston, K. P.; Korgel, B. A. Highly Luminescent Silicon Nanocrystals with Discrete Optical Transitions. *J. Am. Chem. Soc.* **2001**, *123*, 3743–3748.
- (33) Mangolini, L.; Jurbergs, D.; Rogojina, E.; Kortshagen, U. Plasma Synthesis and Liquid-Phase Surface Passivation of Brightly Luminescent Si Nanocrystals. *J. Lumin.* **2006**, *121*, 327–334.
- (34) Mangolini, L.; Jurbergs, D.; Rogojina, E.; Kortshagen, U. High Efficiency Photoluminescence from Silicon Nanocrystals Prepared by Plasma Synthesis and Organic Surface Passivation. *Phys. Status Solidi C* **2006**, *3*, 3975–3978.
- (35) Li, X.; He, Y.; Talukdar, S. S.; Swihart, M. T. Process for Preparing Macroscopic Quantities of Brightly Photoluminescent Silicon Nanoparticles with Emission Spanning the Visible Spectrum. *Langmuir* **2003**, *19*, 8490–8496.
- (36) Belomoin, G.; Therrien, J.; Smith, A.; Rao, S.; Twesten, R.; Chaieb, S.; Nayfeh, M.; Wagner, L.; Mitas, L. Observation of a Magic Discrete Family of Ultrabright Si Nanoparticles. *Appl. Phys. Lett.* **2002**, *80*, 841–843.
- (37) Bley, R. A.; Kauzlarich, S. M.; Davis, J. E.; Lee, H. W. Characterization of Silicon Nanoparticles Prepared from Porous Silicon. *Chem. Mater.* **1996**, *8*, 1881–1888.
- (38) Shen, T.; Koch, C. C.; McCormick, T.; Nemanich, R.; Huang, J.; Huang, J. The Structure and Property Characteristics of Amorphous/Nanocrystalline Silicon Produced by Ball Milling. *J. Mater. Res.* **1995**, *10*, 139–148.
- (39) Heintz, A. S.; Fink, M. J.; Mitchell, B. S. Mechanochemical Synthesis of Blue Luminescent Alkyl/Alkenyl-Passivated Silicon Nanoparticles. *Adv. Mater.* **2007**, *19*, 3984–3988.
- (40) Heintz, A. S.; Fink, M. J.; Mitchell, B. S. Silicon Nanoparticles with Chemically Tailored Surfaces. *Appl. Organomet. Chem.* **2010**, *24*, 236–240.
- (41) Rodríguez, J.; Veinot, J. G. Realization of Sensitized Erbium Luminescence in Si–Nanocrystal Composites Obtained from Solution Processable Sol–Gel Derived Materials. *J. Mater. Chem.* **2011**, *21*, 1713–1720.
- (42) Hessel, C. M.; Henderson, E. J.; Veinot, J. G. An Investigation of the Formation and Growth of Oxide-Embedded Silicon Nanocrystals in Hydrogen Silsesquioxane-Derived Nanocomposites. *J. Phys. Chem. C* **2007**, *111*, 6956–6961.
- (43) Hessel, C. M.; Summers, M. A.; Meldrum, A.; Malac, M.; Veinot, J. G. Direct Patterning, Conformal Coating, and Erbium Doping of Luminescent nc-Si/SiO₂ Thin Films from Solution Processable Hydrogen Silsesquioxane. *Adv. Mater.* **2007**, *19*, 3513–3516.
- (44) Liu, S.; Yang, Y.; Sato, S.; Kimura, K. Enhanced Photoluminescence from Si Nano-Organosols by Functionalization with Alkenes and their Size Evolution. *Chem. Mater.* **2006**, *18*, 637–642.
- (45) Mastronardi, M. L.; Maier-Flaig, F.; Faulkner, D.; Henderson, E. J.; Kübel, C.; Lemmer, U.; Ozin, G. A. Size-Dependent Absolute Quantum Yields for Size-Separated Colloidally-Stable Silicon Nanocrystals. *Nano Lett.* **2012**, *12*, 337–342.
- (46) Manhat, B. A.; Brown, A. L.; Black, L. A.; Ross, J. A.; Fichter, K.; Vu, T.; Richman, E.; Goforth, A. M. One-Step Melt Synthesis of Water-Soluble, Photoluminescent, Surface-Oxidized Silicon Nanoparticles for Cellular Imaging Applications. *Chem. Mater.* **2011**, *23*, 2407–2418.
- (47) Baldwin, R. K.; Pettigrew, K. A.; Garno, J. C.; Power, P. P.; Liu, G.; Kauzlarich, S. M. Room Temperature Solution Synthesis of Alkyl-Capped Tetrahedral Shaped Silicon Nanocrystals. *J. Am. Chem. Soc.* **2002**, *124*, 1150–1151.
- (48) Gupta, A.; Swihart, M. T.; Wiggers, H. Luminescent Colloidal Dispersion of Silicon Quantum Dots from Microwave Plasma Synthesis: Exploring the Photoluminescence Behavior Across the Visible Spectrum. *Adv. Funct. Mater.* **2009**, *19*, 696–703.
- (49) Tilley, R. D.; Yamamoto, K. The Microemulsion Synthesis of Hydrophobic and Hydrophilic Silicon Nanocrystals. *Adv. Mater.* **2006**, *18*, 2053–2056.
- (50) Balagurov, L.; Leiferov, B.; Petrova, E.; Orlov, A.; Panasenko, E. Influence of Water and Alcohols on Photoluminescence of Porous Silicon. *J. Appl. Phys.* **1996**, *79*, 7143–7147.
- (51) Clark, R. J.; Dang, M. K.; Veinot, J. G. Exploration of Organic Acid Chain Length on Water-Soluble Silicon Quantum Dot Surfaces. *Langmuir* **2010**, *26*, 15657–15664.
- (52) Dasog, M.; De los Reyes, G. B.; Titova, L. V.; Hegmann, F. A.; Veinot, J. G. Size vs Surface: Tuning the Photoluminescence of Freestanding Silicon Nanocrystals Across the Visible Spectrum via Surface Groups. *ACS Nano* **2014**, *8*, 9636–9648.
- (53) Dasog, M.; Veinot, J. G. Size Independent Blue Luminescence in Nitrogen Passivated Silicon Nanocrystals. *Phys. Status Solidi A* **2012**, *209*, 1844–1846.
- (54) Dasog, M.; Yang, Z.; Regli, S.; Atkins, T. M.; Faramus, A.; Singh, M. P.; Muthuswamy, E.; Kauzlarich, S. M.; Tilley, R. D.; Veinot, J. G. Chemical Insight into the Origin of Red and Blue Photoluminescence

Arising from Freestanding Silicon Nanocrystals. *ACS Nano* **2013**, *7*, 2676–2685.

(55) Barrelet, C. J.; Robinson, D. B.; Cheng, J.; Hunt, T. P.; Quate, C. F.; Chidsey, C. E. Surface Characterization and Electrochemical Properties of Alkyl, Fluorinated Alkyl, and Alkoxy Monolayers on Silicon. *Langmuir* **2001**, *17*, 3460–3465.

(56) Buriak, J. M.; Allen, M. J. Lewis Acid Mediated Functionalization of Porous Silicon with Substituted Alkenes and Alkynes. *J. Am. Chem. Soc.* **1998**, *120*, 1339–1340.

(57) Stewart, M. P.; Buriak, J. M. Photopatterned Hydrosilylation on Porous Silicon. *Angew. Chem., Int. Ed.* **1998**, *37*, 3257–3260.

(58) Littau, K.; Szajowski, P.; Muller, A.; Kortan, A.; Brus, L. A Luminescent Silicon Nanocrystal Colloid via a High-Temperature Aerosol Reaction. *J. Phys. Chem.* **1993**, *97*, 1224–1230.

(59) Schuppler, S.; Friedman, S.; Marcus, M.; Adler, D.; Xie, Y.; Ross, F.; Harris, T.; Brown, W.; Chabal, Y.; Brus, L.; Citrin, P. H. Dimensions of Luminescent Oxidized and Porous Silicon Structures. *Phys. Rev. Lett.* **1994**, *72*, 2648–2651.

(60) Wolkin, M.; Jorne, J.; Fauchet, P.; Allan, G.; Delerue, C. Electronic States and Luminescence in Porous Silicon Quantum Dots: The Role of Oxygen. *Phys. Rev. Lett.* **1999**, *82*, 197–200.

(61) Angi, A.; Sinelnikov, R.; Meldrum, A.; Veinot, J. G.; Balberg, I.; Azulay, D.; Millo, O.; Rieger, B. Photoluminescence through In-Gap States in Phenylacetylene Functionalized Silicon Nanocrystals. *Nanoscale* **2016**, *8*, 7849–7853.

(62) Höhlein, I.; Angi, A.; Sinelnikov, R.; Veinot, J. G.; Rieger, B. Functionalization of Hydride-Terminated Photoluminescent Silicon Nanocrystals with Organolithium Reagents. *Chem. - Eur. J.* **2015**, *21*, 2755–2758.

(63) Dohnalová, K.; Gregorkiewicz, T.; Kúsová, K. Silicon Quantum Dots: Surface Matters. *J. Phys.: Condens. Matter* **2014**, *26*, 173201–173228.

(64) Li, X.; He, Y.; Swihart, M. T. Surface Functionalization of Silicon Nanoparticles Produced by Laser-Driven Pyrolysis of Silane Followed by HF-HNO₃ etching. *Langmuir* **2004**, *20*, 4720–4727.

(65) Yang, Z.; Iqbal, M.; Dobbie, A. R.; Veinot, J. G. Surface-Induced Alkene Oligomerization: Does Thermal Hydrosilylation Really Lead to Monolayer Protected Silicon Nanocrystals? *J. Am. Chem. Soc.* **2013**, *135*, 17595–17601.

(66) Kelly, J. A.; Veinot, J. G. An Investigation into Near-UV Hydrosilylation of Freestanding Silicon Nanocrystals. *ACS Nano* **2010**, *4*, 4645–4656.

(67) Purkait, T. K.; Iqbal, M.; Wahl, M. H.; Gottschling, K.; Gonzalez, C. M.; Islam, M. A.; Veinot, J. G. Borane-Catalyzed Room-Temperature Hydrosilylation of Alkenes/Alkynes on Silicon Nanocrystal Surfaces. *J. Am. Chem. Soc.* **2014**, *136*, 17914–17917.

(68) Höhlein, I.; Kehrle, J.; Helbich, T.; Yang, Z.; Veinot, J. G.; Rieger, B. Diazonium Salts as Grafting Agents and Efficient Radical-Hydrosilylation Initiators for Freestanding Photoluminescent Silicon Nanocrystals. *Chem. - Eur. J.* **2014**, *20*, 4212–4216.

(69) Yang, Z.; Gonzalez, C. M.; Purkait, T. K.; Iqbal, M.; Meldrum, A.; Veinot, J. G. Radical Initiated Hydrosilylation on Silicon Nanocrystal Surfaces: An Evaluation of Functional Group Tolerance and Mechanistic Study. *Langmuir* **2015**, *31*, 10540–10548.

(70) Bell, J. P.; Cloud, J. E.; Cheng, J.; Ngo, C.; Kodambaka, S.; Sellinger, A.; Williams, S. K. R.; Yang, Y. N-Bromosuccinimide-Based Bromination and Subsequent Functionalization of Hydrogen-Terminated Silicon quantum dots. *RSC Adv.* **2014**, *4*, 51105–51110.

(71) Maier-Flaig, F.; Rinck, J.; Stephan, M.; Bocksrocker, T.; Bruns, M.; Kübel, C.; Powell, A. K.; Ozin, G. A.; Lemmer, U. Multicolor Silicon Light-Emitting Diodes (SiLEDs). *Nano Lett.* **2013**, *13*, 475–480.

(72) Yu, Y.; Bosoy, C. A.; Smilgies, D.; Korgel, B. A.; Self-Assembly and Thermal Stability of Binary Superlattices of Gold and Silicon Nanocrystals. *J. Phys. Chem. Lett.* **2013**, *4*, 3677–3682.

(73) Nguyen, A.; Gonzalez, C. M.; Sinelnikov, R.; Newman, W.; Sun, S.; Lockwood, R.; Veinot, J. G.; Meldrum, A. Detection of Nitroaromatics in the Solid, Solution, and Vapor Phases using Silicon Quantum Dot Sensors. *Nanotechnology* **2016**, *27*, 105501–105512.

(74) Kehrle, J.; Höhlein, I.; Yang, Z.; Jochem, A.; Helbich, T.; Kraus, T.; Veinot, J. G.; Rieger, B. Thermoresponsive and Photoluminescent Hybrid Silicon Nanoparticles by Surface-Initiated Group Transfer Polymerization of Diethyl Vinylphosphonate. *Angew. Chem.* **2014**, *126*, 12702–12705.

(75) Guidelines for Safe Use of Hydrofluoric Acid (HF). <https://www.ualberta.ca/environment-health-safety/self-help/document-cabinet> (accessed June 29, 2016).

(76) Song, J.; Chen, S.; Zhou, M.; Xu, T.; Lv, D.; Gordin, M. L.; Long, T.; Melnyk, M.; Wang, D. Micro-Sized Silicon-Carbon Composites Composed of Carbon-Coated Sub-10 nm Si Primary Particles as High-Performance Anode Materials for Lithium Ion Batteries. *J. Mater. Chem. A* **2014**, *2*, 1257–1262.

(77) Purkait, T. K.; Iqbal, M.; Islam, M. A.; Mobarok, M. H.; Gonzalez, C. M.; Hadidi, L.; Veinot, J. G. Alkoxy-Terminated Si Surfaces: A New Reactive Platform for the Functionalization and Derivatization of Silicon Quantum Dots. *J. Am. Chem. Soc.* **2016**, *138*, 7114–7120.

(78) Höhlein, I. M.; Kehrle, J.; Purkait, T. K.; Veinot, J. G.; Rieger, B. Photoluminescent Silicon Nanocrystals with Chlorosilane Surfaces—Synthesis and Reactivity. *Nanoscale* **2015**, *7*, 914–918.

(79) Warner, J. H.; Hoshino, A.; Yamamoto, K.; Tilley, R. Water-Soluble Photoluminescent Silicon Quantum Dots. *Angew. Chem.* **2005**, *117*, 4626–4630.

(80) Yu, Y.; Rowland, C. E.; Schaller, R. D.; Korgel, B. A. Synthesis and Ligand Exchange of Thiol-Capped Silicon Nanocrystals. *Langmuir* **2015**, *31*, 6886–6893.

(81) Hessel, C. M.; Rasch, M. R.; Hueso, J. L.; Goodfellow, B. W.; Akhavan, V. A.; Puvanakrishnan, P.; Tunnel, J. W.; Korgel, B. A. Alkyl Passivation and Amphiphilic Polymer Coating of Silicon Nanocrystals for Diagnostic Imaging. *Small* **2010**, *6*, 2026–2034.

(82) Yu, Y.; Hessel, C. M.; Bogart, T. D.; Panthani, M. G.; Rasch, M. R.; Korgel, B. A. Room Temperature Hydrosilylation of Silicon Nanocrystals with Bifunctional Terminal Alkenes. *Langmuir* **2013**, *29*, 1533–1540.

(83) Yang, Z.; Dasog, M.; Dobbie, A. R.; Lockwood, R.; Zhi, Y.; Meldrum, A.; Veinot, J. G. Highly Luminescent Covalently Linked Silicon Nanocrystal/Polystyrene Hybrid Functional Materials: Synthesis, Properties, and Processability. *Adv. Funct. Mater.* **2014**, *24*, 1345–1353.

(84) Yu, Y.; Korgel, B. A. Controlled Styrene Monolayer Capping of Silicon Nanocrystals by Room Temperature Hydrosilylation. *Langmuir* **2015**, *31*, 6532–6537.

(85) Murphy, C. J.; Buriak, J. M. Best Practices for the Reporting of Colloidal Inorganic Nanomaterials. *Chem. Mater.* **2015**, *27*, 4911–4913.

(86) Henderson, E. J.; Kelly, J. A.; Veinot, J. G. Influence of HSiO_{1.5} Sol–Gel Polymer Structure and Composition on the Size and Luminescent Properties of Silicon Nanocrystals. *Chem. Mater.* **2009**, *21*, 5426–5434.

(87) CasaXPS: Processing Software for XPS, AES, SIMS and More. <http://www.casaxps.com/> (accessed June 29, 2016).

(88) ImageJ: An Open Platform for Scientific Image Analysis. <http://imagej.net/Welcome> (accessed June 29, 2016).